

High-temperature elasticity and viscosity of $\text{Ge}_x\text{Se}_{1-x}$ glasses in the transition rangeYann Gueguen,¹ Tanguy Rouxel,^{1,*} Pascal Gadaud,² Cedric Bernard,^{1,†}
Vincent Keryvin,^{1,†} and Jean-Christophe Sangleboeuf¹¹LARMAUR ERL-CNRS 6274, Université Rennes 1, Bat. 10 B, Campus de Beaulieu, 35042 Rennes Cedex, France²Laboratoire de Mécanique et Physique des Matériaux, CNRS UMR 6617, ENSMA, 1 Avenue Clément Ader, BP 40109, F-86961 Futuroscope Cedex, France

(Received 16 July 2010; revised manuscript received 19 May 2011; published 17 August 2011)

The viscous-flow behavior and temperature dependence of the elastic moduli of chalcogenide glasses from the germanium-selenium system were studied by means of homemade high-temperature indentation setup and resonant-frequency technique (1–10 kHz), respectively, for temperatures between 0.8 and $1.2 \times T_g$. The softening rates, both in the elastic and in the viscous-flow regimes, were correlated to network deconstruction or reorganization events in the light of previously reported high-temperature neutron-scattering data. The concomitant change of Poisson's ratio (ν) and the thermodynamic parameters of the thermally activated viscous-flow process were characterized and provide a new basis for the understanding of the sources for the softening in the transition range. The temperature dependence of ν suggests weak changes of the network cross-linking degree at large Ge contents. On the contrary, in the case of a-Se, a steep fragmentation of the structural units is inferred from the $\nu(T)$ data, and the flow process is accompanied by a huge entropy change (activation entropy at saddle point). The entropy contribution at T_g ($T_g \times \Delta S_a$) represents more than 50% of the activation enthalpy for flow (ΔH_a) and increases with the selenium content. Hence the free activation energy (ΔG_a) is much smaller than apparent activation energy as derived from viscosity data.

DOI: [10.1103/PhysRevB.84.064201](https://doi.org/10.1103/PhysRevB.84.064201)

PACS number(s): 61.43.Fs, 62.20.de, 62.20.dj, 66.20.Ej

I. INTRODUCTION

Glasses from the germanium-selenium system have already been extensively studied both because of their excellent transparency in the far infrared wavelengths range and because they show up as model binary covalent glasses.^{1–4} However, the incidence of temperature on their properties is a critical issue, especially for the most chalcogen-rich compositions, which exhibit glass-transition temperature below 350 K. It is of paramount interest not only at the processing and shaping stages but also to evaluate the stability of glass parts in service conditions.

Elastic moduli are intimately related to volume density of energy⁵ and to the network connectivity ($\langle n \rangle$)^{6,7} [in the case of $\text{Ge}_x\text{Se}_{1-x}$ glasses, $\langle n \rangle = 2(x + 1)$].⁸ As long as $\langle n \rangle$ is less than 2.1, the selenium chains (or rings) are weakly interconnected so that deformation is expected to essentially proceed through the alignment of the chains in shear planes. In this case properties are believed to be very sensitive to the weak interchains Van der Waals forces. A low shear resistance and a high Poisson's ratio follow. As $\langle n \rangle$ increases, covalent bonds come into play. At first sight, $\langle n \rangle = 2.4$ (GeSe_4 composition) corresponds to a complete cross-linking of Se and Ge layer units, two neighboring Ge atoms being separated by two Se atoms on average. At $\langle n \rangle = 2.67$ (GeSe_2 stoichiometry), homopolar Ge-Ge are present, and a three-dimensional network is found, leading to a significant increase of the elastic moduli and of the viscosity,^{7–9} which can be viewed as a result of stressed rigidity.¹⁰ The structure of these glasses might be slightly more complicated though (as will be further discussed) with Se occurring in at least three different sites¹¹ and possible “clustering” at the scale of the structural units.^{12–19} Most studies published over the last two years agree that the structure of Ge-Se glasses significantly differs from the one predicted

by the simple chain crossing and outrigger raft models,¹⁷ and very recent ⁷⁷Se NMR investigations demonstrated^{18,19} the existence of Se-**Se**-Ge fragments connecting GeSe_2 clusters and Se chains domains. Although elastic moduli (continuum scale measurement) are essentially independent of the fine details of the network structure, the possible coexistence of soft and stiff regions will surely affect the temperature dependence through a “composite”-like effect which can be probed by means of high temperature measurements. Besides, elasticity data obtained in the temperature range for viscosity measurements allow for the derivation of the actual values for the activation energy and the free activation energy for flow from the directly available (apparent) heat of flow (enthalpy). The combination of elasticity and viscosity data thus provides a unique opportunity to get insight into the flow mechanisms and into the composition sensitivity of the rheological behavior.

II. MATERIALS AND EXPERIMENTAL METHODS**A. Materials**

$\text{Ge}_x\text{Se}_{1-x}$ glasses, with x between 0 and 0.3, were obtained from high purity elements Ge (99.9999%) and Se (99.999%). Se was further purified of remaining oxygen by the volatilization technique, consisting in heating Se at 523 K under vacuum for 2 hours. This method uses the greater vapor pressure of selenium oxide SeO_2 over that of the metal to remove the oxide species. Proper amounts of Ge and Se are subsequently introduced into an amorphous silica tube sealed in vacuum with better than 10^{-2} -Pa pressure in order to avoid oxygen contamination. The sealed silica tube was introduced into a rocking furnace and kept at 1023 K for 12 hours to ensure a good mixing and homogenization of the liquid. The temperature was subsequently reduced to 923 K and staid constant for 1 hour to reduce the gas pressure in the tube.^{3,12,13} The obtained

glass melt was then quenched in water (293 K) and annealed at T_g for 4 hours to reduce the residual stresses resulting from the cooling. The glass rod was sliced and cut to the desired mechanical testing specimen geometry using a diamond saw. Surfaces of the specimens were mirror polished using SiC paper and alumina suspension (1/4-micron particle size).

The glass-transition temperature T_g was measured by a TA Instrument differential scanning calorimetry (DSC) Q20, with a heating rate of 10 K/min, with a better than ± 2 K accuracy. The density was measured at 293 K using the Archimedes displacement technique using CCl_4 . The variability of such a measurement is approximately $\pm 0.5\%$.

B. Experimental methods

Our laboratory has developed equipment operating in the microindentation range, with applied loads between 0.01 and 15 N, consisting in a hot chamber equipped with an alumina tube and a sapphire indenter and allowing for a better than 2 K accuracy along a 10-mm-testing zone.^{20,21} The whole equipment is situated in a vibration-free and air-disturbance-free environment. The load is applied using a piezoelectric actuator, and the penetration depth is measured with a capacitive sensor having a resolution of 10 nm. The load fluctuation is less than ± 12 mN. The maximum target temperature is 1473 K with a thermal stability within 1 K with a variation up to 1323 K.

The shear viscosity coefficient (η) was estimated from indentation experiments performed at a constant load (P) of 12.5 N in air using a ball indenter [750 μm radius (R)] and is given by²¹⁻²³

$$\eta = \frac{3P}{16\sqrt{R}} \left(\frac{d(u^{3/2}(t))}{dt} \right)^{-1}, \quad (1)$$

where u is the penetration depth.

Recall that the viscous flow regime is associated to the stationary creep regime following the viscoelastic transient one. Consequently the load was maintained long enough (typically 1 min above T_g to more than 1 hour for points recorded below T_g) to ensure the occurrence of a stationary creep regime, as evidenced by a constant slope in the $u^{3/2}/P$ versus t curves. This problem is particularly critical as soon as measurements are carried out below T_g , i.e., in a range where the characteristic relaxation time increases rapidly and compares with the experimental duration. The specimen and the indentation set-up were kept at each testing temperature for up to 4 hours before loading to ensure a thermal equilibrium.

Young's modulus was determined by means of a resonant frequency technique in bending mode in the kHz range.²⁴ This method allows us to perform experiments at $1 \text{ K} \cdot \text{mn}^{-1}$ under high vacuum (10^{-4} Pa) up to 1300 K without any harmful contact, the sample beam being maintained horizontally between steel wires located at the vibration nodes. Furthermore, excitation and detection are insured by an electrostatic device (capacitance created between the sample and a single electrode). The accuracy of this method is better

than 0.5% for conducting bulk materials whatever the rigidity range. Young's modulus (E) is expressed as²⁴

$$E = 0.9464 \rho F_B^2 \left[\frac{L^4(t)}{h^2} T(h/L, \nu) \right], \quad (2)$$

where F_B is the resonance frequency in bending mode, ρ the specific mass, ν Poisson's ratio, h and L the beam thickness and span length, and $T(h/L, \nu)$ a correcting factor close to 1.

For this work, $20 \times 4 \times 2$ -mm³-parallelepipedic bars were plated on one face (AuPd-metallic-vapor deposition of about 10-nm thick) in order to be electrostatically excited.

A new testing head has been designed in agreement with ASTM recommendations to determine the shear modulus (μ) of plates (typically 30 mm \times 12 mm \times 1.5 mm) in torsion mode,²⁵

$$\mu = \frac{4\rho}{RL^2 F_T^2}, \quad (3)$$

where R is a shape factor equal to 17.51 in the present case, ρ is the specific mass, L is the length of the plate-like specimen, and F_T is the torsion resonant frequency.

III. RESULTS

Owing to the experimental difficulty to assess high-temperature elasticity data, and especially because of the machining of specimens in such brittle glasses (fracture toughness of GeSe glasses is typically below $0.3 \text{ MPa} \cdot \text{m}^{0.5}$), measurements were limited to a-Se, GeSe₄, GeSe₃, and Ge₃Se₇ compositions (Fig. 1). Additional investigations focused on Young's modulus were previously reported by Gadaud *et al.*²⁴

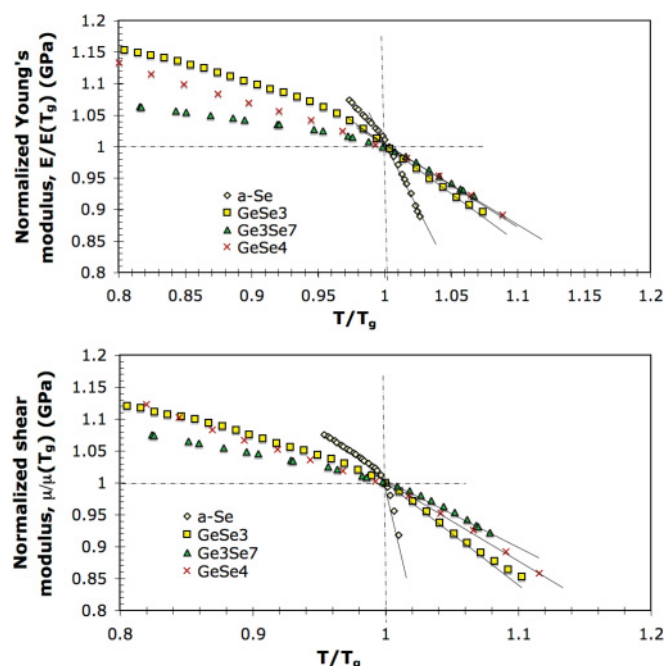


FIG. 1. (Color online) (a) Temperature dependence of Young's modulus (E). (b) Temperature dependence of the shear modulus (μ). Note the rapid decrease of the shear modulus in a-Se for $T > T_g$, which contrasts with the decrease found for E .

TABLE I. Measurements of elastic moduli and shear viscosity coefficient as a function of temperature. x: Nonmeasured.

T/T_g^a	a-Se $T_g = 302$ K			GeSe ₄ $T_g = 416$ K			GeSe ₃ $T_g = 498$ K			Ge ₃ Se ₇ $T_g = 579$ K		
	E (GPa)	μ (GPa)	\log_{10} (Pa · s)	E (GPa)	μ (GPa)	$\log_{10} \eta$ (Pa · s)	E (GPa)	μ (GPa)	$\log_{10} \eta$ (Pa · s)	E (GPa)	μ (GPa)	$\log_{10} \eta$ (Pa · s)
0.930	x	x	x	12.45	5.06	14.69	14.07	5.60	x	16.40	6.51	x
0.935	x	x	x	12.41	5.04	14.56	14.02	5.58	x	16.38	6.50	x
0.940	x	x	x	12.37	5.03	14.43	13.96	5.56	x	16.35	6.48	x
0.945	x	x	x	12.33	5.01	14.30	13.90	5.54	x	16.32	6.47	x
0.950	x	x	x	12.30	4.99	14.17	13.84	5.52	x	16.29	6.46	13.71
0.955	x	x	x	12.26	4.98	14.04	13.78	5.50	x	16.26	6.45	13.61
0.960	x	x	x	12.23	4.97	13.91	13.72	5.48	x	16.23	6.43	13.51
0.965	x	x	x	12.19	4.95	13.78	13.65	5.46	x	16.19	6.41	13.40
0.970	9.65	3.87	13.71	12.15	4.93	13.65	13.58	5.44	13.10	16.15	6.40	13.29
0.973	9.60	3.86	13.51	12.13	4.92	13.57	13.54	5.43	13.02	16.13	6.39	13.22
0.976	9.54	3.85	13.32	12.11	4.91	13.49	13.50	5.42	12.94	16.10	6.38	13.15
0.979	9.49	3.83	13.13	12.09	4.90	13.41	13.45	5.41	12.86	16.08	6.38	13.08
0.982	9.43	3.82	12.94	12.07	4.88	13.34	13.41	5.40	12.78	16.05	6.37	13.00
0.985	9.36	3.80	12.74	12.05	4.87	13.26	13.36	5.38	12.69	16.03	6.36	12.93
0.988	9.30	3.78	12.55	12.03	4.86	13.18	13.32	5.37	12.61	16.00	6.35	12.85
0.991	9.23	3.76	12.36	12.00	4.85	13.10	13.27	5.36	12.53	15.97	6.34	12.78
0.994	9.16	3.71	12.17	11.98	4.83	13.02	13.22	5.35	12.45	15.94	6.32	12.70
0.997	9.09	3.71	11.97	11.96	4.82	12.95	13.18	5.33	12.37	15.90	6.31	12.62
1.000	9.00	3.67	11.78	11.88	4.81	12.87	13.00	5.30	12.29	15.89	6.30	12.54
1.003	8.89	3.60	11.59	11.84	4.80	12.79	12.94	5.27	12.21	15.84	6.29	12.46
1.006	8.77	3.51	11.40	11.81	4.78	12.71	12.88	5.24	12.13	15.78	6.27	12.38
1.009	8.65	3.40	11.20	11.77	4.77	12.64	12.82	5.22	12.06	15.73	6.26	12.30
1.012	8.52	3.27	11.01	11.74	4.75	12.56	12.75	5.19	11.98	15.68	6.25	12.21
1.015	8.39	3.12	10.82	11.70	4.74	12.48	12.69	5.16	11.90	15.62	6.23	12.13
1.018	8.25	2.97	10.63	11.66	4.73	12.40	12.63	5.14	11.82	15.57	6.22	12.05
1.021	8.11	2.81	10.43	11.63	4.71	12.33	12.57	5.11	11.74	15.52	6.20	11.96
1.024	7.96	2.65	10.24	11.59	4.70	12.25	12.51	5.09	11.67	15.46	6.19	11.88
1.027	7.80	2.50	10.05	11.55	4.68	12.17	12.46	5.06	11.59	15.41	6.17	11.79
1.030	7.65	2.36	9.85	11.51	4.67	12.09	12.40	5.04	11.52	15.35	6.15	11.71
1.033	7.48	2.22	9.66	11.47	4.65	12.02	12.34	5.01	11.44	15.30	6.14	11.62
1.040	x	x	9.21	11.37	4.61	11.84	12.21	4.96	11.26	15.17	6.09	11.42
1.060	x	x	x	11.08	4.50	11.32	11.84	4.80	10.77	14.78	5.96	10.85
1.080	x	x	x	10.76	4.38	10.81	11.50	4.65	10.30	14.38	5.81	10.30
1.100	x	x	x	x	x	10.30	11.17	4.51	9.84	13.96	5.64	9.79
1.120	x	x	x	x	x	9.79	x	x	9.40	x	x	9.33
1.140	x	x	x	x	x	9.28	x	x	8.97	x	x	8.95
1.160	x	x	x	x	x	x	x	x	8.56	x	x	8.66

^aAs determined from the $E(T)$ curves (Table II).

for Ge₁₅Se₈₅ and Ge₃Se₇ compositions. The raw measurements of E , μ , and η are reported in Table I (note that these data might be further used to estimate the vibrational entropy of both the glass and the supercooled liquids from the classical assumption that S_{vib} is proportional to $d\mu/dT$).

The elastic moduli exhibit only minor changes between room temperature (RT) and T_g . Their values at T_g are more than 80% of their RT values. With regard to the considered temperature interval (0.8 to 1.1 T_g), data in the supercooled-liquid region exhibit a linear dependence with temperature. The $\frac{dE}{dT}|_{T \geq T_g}$ and $\frac{d\mu}{dT}|_{T \geq T_g}$ slopes are reported together with the transition temperatures and the corresponding values of the elastic moduli in Table II. In all cases experimental data exhibit a change of the softening rate in a temperature range corresponding within 15°C of the glass-transition temperature as obtained by classical means such as Differential Scanning

Calorimetry (DSC) and dilatometry. In the case of a-Se the transition observed in shear lies about 7 K below that observed in the $E(T)$ curve. For reasons that have not yet been elucidated, the transition as observed from elasticity data is shifted to lower temperature, notwithstanding the fact that frequencies in the 1 to 10 kHz range were used. A similar observation on glasses from various systems and using a different experimental set-up was previously reported.⁷ Nevertheless, since a clear transition between two regimes was always observed in a temperature range quite close to the one identified as the T_g range by DSC, this transition was considered in this work to be the glass-transition range with respect to the used technique. The softening rate of a-Se above T_g ($-115 \text{ MPa} \cdot \text{K}^{-1}$) is close to the one reported for Zr-based metallic glasses²⁶ or oxynitride glasses,²⁷ but is approximately twice less than that for glycerol ($\sim -190 \text{ MPa} \cdot \text{K}^{-1}$).²⁸ The

addition of germanium results in a significant reinforcement of the glass. With more than 25 at.% germanium, the softening rate (in absolute value) becomes three to four times smaller. The viscosity curves as obtained by instrumented indentation are plotted together with previously published data^{29–33} on glasses with the same compositions as in Fig. 2(a). The indentation method allows us to cover a broad range of viscosity values on both sides of T_g , with a unique opportunity to probe the low temperature range associated with viscosities above 10^{13} Pa·s. It is noteworthy that the present data are in excellent agreement with those reported in the literature for $T > T_g$. There are five to six orders of magnitude differences in the viscosity coefficients at a given temperature between adjacent curved, i.e., as the germanium content changes by about 10%.

In the following sections we will discuss the viscous-flow process in the light of general concepts developed in the framework of thermally activated processes regardless of any structural or microscopical ingredients. With regard to the viscosity range considered here—for η between 10^8 and 10^{15} Pa·s—the experimental data could be expressed with a smooth curve fitting as a function of temperature using a

classical Boltzmann term accounting for the probability of a given fluctuation to overcome the relevant energy barrier,

$$\eta = \eta_0 \exp[G_a/(RT)], \quad (4)$$

where η_0 is a temperature-independent factor, R is the perfect gas constant, and ΔG_a is the free activation enthalpy for flow.

However, it must be emphasized that ΔG_a is by essence a temperature-dependent parameter (differentiation of the free enthalpy with respect to T is the negative of the entropy), so that the derivation of Eq. (4) with respect to temperature leads to

$$R \left. \frac{\partial \ln \eta}{\partial (1/T)} \right|_{\sigma} = \Delta G_a - T \left. \frac{\partial \Delta G_a}{\partial T} \right|_{\sigma} = \Delta G_a - T \Delta S_a \quad (5)$$

where σ is the stress applied on the specimen (see Refs. 34 and 35 for further background on this analysis) and is mentioned here to recall that T and σ are the two independent external variables in this problem.

In the analogy with the formalism introduced in Chemical Kinetics,³⁶ ΔS_a can be considered as the entropy of activation of the flow process. Hence, it is inferred from Eqs. (4) and (5) that the only directly available experimental parameter is the activation enthalpy (heat of flow),

$$H_a = \left. \frac{\partial \ln \eta}{\partial (1/T)} \right|_{\sigma}. \quad (6)$$

ΔH_a values as determined from the slope of the linear intercepts in Fig. 2(b) are reported in Table III. Following the classical theory of thermally activated flow phenomena, it is possible to estimate ΔG_a once the temperature dependence of the shear modulus is known [two important assumptions here are (i) the height of the energy barrier is proportional to the shear modulus, and (ii) the contribution of the mechanical work to overcome the barrier is small in comparison to that of thermal activation],^{34,35,37}

$$\Delta G_a = \frac{\Delta H_a}{1 - \frac{T}{\mu} \frac{\partial \mu}{\partial T}}. \quad (7)$$

The activation entropy is then given by $\Delta S_a = (\Delta H_a - \Delta G_a)/T$:

$$\Delta S_a = \frac{\frac{1}{\mu} \frac{\partial \mu}{\partial T}}{\frac{T}{\mu} \frac{\partial \mu}{\partial T} - 1} \Delta H_a. \quad (8)$$

Another approach was proposed by Nemilov,³⁸ assuming that all viscosity curves meet in the supercooled-liquid region at a given T_g/T ratio corresponding to a viscosity of about $10^{-4.5}$ Pa·s. In this latter approach both ΔG_a and ΔS_a are solely estimated from the viscosity data on the basis of Eqs. (5) and (6). For instance at T_g it comes that $\Delta S_a = -316 + \Delta H_a/T_g$ and $\Delta G_a(T_g) = 316 T_g$. The activation volume (V_a) associated to the overcoming (saddle point) of the energy barrier for flow is another important parameter. Because $V_a = -\left. \frac{\partial \Delta G_a}{\partial \sigma} \right|_T$, it is in principal required to perform temperature-jump experiments for different values of the applied stress to estimate the activation volume. However Nemilov³⁹ proposed a simple estimation for a volume V^* , considered to be that of kinetic units overcoming the activation barrier, from the free activation enthalpy for flow and from the shear modulus, $V^* = \Delta G_a/\mu$ and concluded that V^*/N (N:

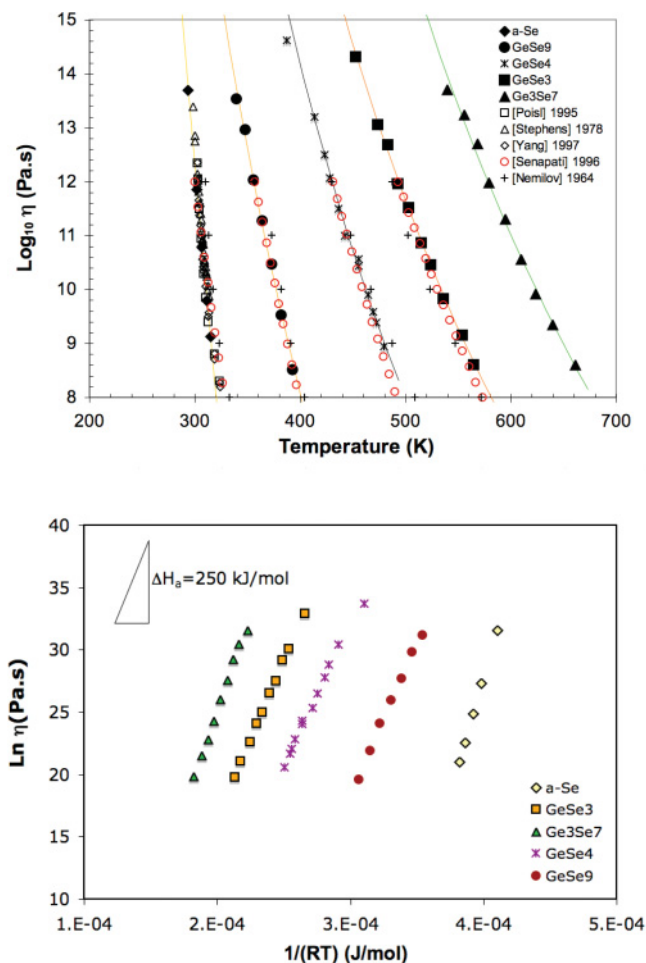


FIG. 2. (Color online) (a) Temperature dependence of the shear viscosity coefficient (η). (b) Determination of the apparent activation energy (ΔH_a) from the viscosity data.

TABLE II. Elastic properties of $\text{Ge}_x\text{Se}_{1-x}$ glasses.

Glass	T_g^a (K)	T_g^b (K)	E_{RT} (GPa)	μ_{RT} (GPa)	ν_{RT}	$E(T_g)$ (GPa)	$\mu(T_g)$ (GPa)	$dE/dT(T_g^+)^c$ (MPa · K ⁻¹)	$d\mu/dT(T_g^+)^c$ (MPa · K ⁻¹)
a-Se	313	302	10.3	3.88	0.322	9.0	3.67	-115	-93.8
GeSe ₄	435	416	14.73	5.73	0.286	11.8	4.81	-35.7	-14.3
GeSe ₃	501	499	16.1	6.26	0.281	13.0	5.30	-38.4	-16.3
Ge ₃ Se ₇	573	579	17.9	7.08	0.264	15.9	6.30	-30.8	-11.3

^aFrom differential scanning calorimetry.

^bTransition temperature observed in the $E(T)$ measurement with the resonant technique.

^cSoftening rates measured in the supercooled-liquid range.

Avogadro number) can be written as r_o^3 where r_o is in excellent agreement (within 10%) with some interatomic distance [see Ref. 39 for details]. A similar expression was obtained by Dyre *et al.*⁴⁰ using a volume expansion model, although in this later case the characteristic volume was given a slightly different meaning.

The values for the parameters of the thermally activated viscous flow process are reported in Table III.

IV. DISCUSSION

The softening of glasses above T_g is chiefly related to the deconstruction of the atomic network. However, the microscopic events at the source for this thermal weakening are quite complicated and differ from one glass to the other. Various scenarios might be invoked depending on the type of structural units and on the interunits bonding. Interestingly, elastic moduli and shear viscosity coefficient are likely to be primarily sensitive to different microscopic features. For instance, Young's modulus expresses the stiffness of the structural units to a normal stress, whereas the shear modulus is more sensitive to the interunit bonding. In principle, elastic moduli are little affected by the size or the length of the structural units, whereas viscosity is very sensitive to their size and shape and to the presence of a continuous softer phase.

A. Network cross linking, average coordination, and elastic behavior

The increase of both E and μ with the germanium content mainly stems from the increase of $\langle n \rangle$. Bridges⁶ and Nemilov³⁹ reported some interesting correlation between Poisson's ratio (ν) and glass-network structures, and ν was found recently

to show up as a remarkable index of the cross-linking degree regardless of the chemical system.⁷ For $\text{Ge}_x\text{Se}_{1-x}$ glasses, a linear relationship (correlation = 0.985) is obtained from previously published elasticity data on the same specimens⁴¹

$$\nu = 0.5135 - 0.0946\langle n \rangle, \quad (9)$$

where $\langle n \rangle$ is the average coordination number. Note that a very close relationship was also reported in the Ge-Sb-Se system.⁸

Although E , μ , and ν change monotonically with $\langle n \rangle$, their temperature dependences are more interesting. For instance, both dE/dT and $d\mu/dT$ (Table II) are larger for the GeSe₃ composition in the supercooled-liquid range (T_g^+) than for the GeSe₄ and Ge₃Se₇ compositions. It is noteworthy that the GeSe₃ composition precisely lies in the so-called intermediate-phase range (after Boolchand *et al.*^{10,42}).

Although it has received little attention so far, the temperature dependence of ν is of paramount interest to probe the thermally induced structural changes in the cross-linking. Recalling that $\nu = E/2\mu - 1$, $\nu(T)$ data were calculated from $E(T)$ and $\mu(T)$ ones (Fig. 3). A perfectly incompressible body is characterized by $\nu = 0.5$ and rubber, glycerol, and Pd-based metallic glasses get very close to this upper bound above their T_g . On the contrary, a-SiO₂ (a tetrahedrally coordinated glass as GeSe₂) retains its cross-linked structure well beyond the T_g range.⁷ In the present case it seems that the cross linking remains strong in both GeSe₃ and Ge₃Se₇ compositions up to $1.1 \times T_g$ whereas a-Se experiences a severe depolymerization and approaches the liquid state in a steep manner. It is noteworthy that for a-Se the increase of ν begins below the T_g range as estimated from $E(T)$ curves. A similar temperature shift was reported earlier on a-Se by Böhmer *et al.*⁹ from ultrasonic investigations in the 1–20 MHz

TABLE III. Viscous flow properties in the transition range of $\text{Ge}_x\text{Se}_{1-x}$ glasses.

Glass	T_g^a (K)	ΔH_a [Eq. (6)] (kJ · mol ⁻¹)	ΔG_a [Eq. (7)] (kJ · mol ⁻¹)	ΔS_a [Eq. (8)] (J · K ⁻¹ · mol ⁻¹)	m^b	ΔG_a^c (kJ · mol ⁻¹)	ΔS_a^c (J · K ⁻¹ · mol ⁻¹)	V^{*c} (m ³ · mol ⁻¹)
a-Se	301	369	41	1090	64	95	910	11.10 ⁻⁶
GeSe ₉	356	249	nd	nd	37	112	383	nd
GeSe ₄	430	243	109	312	30	136	249	23.10 ⁻⁶
GeSe ₃	492	256	101	315	27	155	204	19.10 ⁻⁶
Ge ₃ Se ₇	580	294	144	258	26	183	191	23.10 ⁻⁶

^aTemperature for $\eta = 10^{12}$ Pa · s.

^bAs defined by $m = d \log_{10} \eta / d[T(\eta = 10^{12} \text{ Pa} \cdot \text{s})/T] = \Delta H_a / (2.303 RT_g)$.⁴³

^c ΔG_a measured near T_g . From the approach proposed by Nemilov.^{33,34} nd: nondetermined.

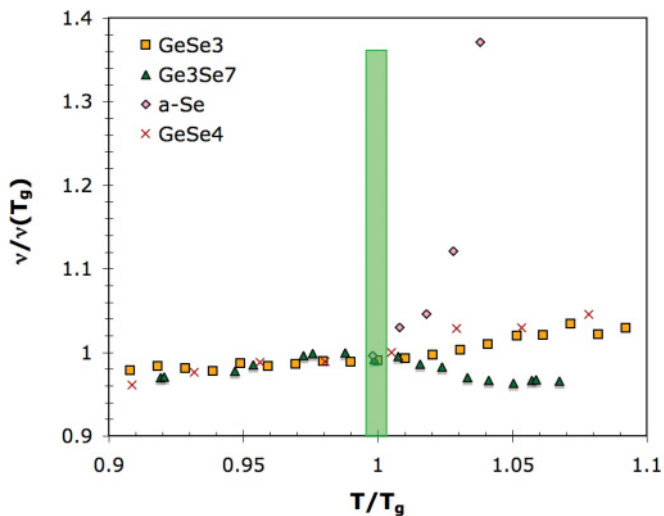


FIG. 3. (Color online) Temperature dependence of Poisson's ratio [note that temperature is normalized to T_g as estimated from the $E(T)$ data].

range. The excitation frequencies used here are close to 5 and 8 kHz, and the corresponding periods ($1-2 \cdot 10^{-4}$ s) are thus hundreds of times smaller than the characteristic relaxation time (η/μ from the Maxwell model), which is larger than 5 min below T_g . Therefore it doesn't seem reasonable to invoke any dynamic effect, in accord with Böhmer's conclusion,⁹ nor to account for the dynamic Poisson's ratio.⁴³ A possible explanation is that the weak interchain bonding (major contribution to μ) collapses at a lower temperature than the covalent bonds. The fragmentation of the chains may also weaken the shear resistance more than the uniaxial stiffness. However, the elasticity measurements on a-Se should be taken with caution for the following reasons: (i) Dynamic structural relaxation might occur during loading attributable to a T_g range close to ambient temperature; and (ii) the ± 2 K accuracy of our equipment might be a problem for the calculation of ν of low T_g glasses because small temperature differences induce a dramatic deviation in ν .

Now let us summarize what we can learn from the literature about thermally induced structural changes in the studied glasses. a-Se is often considered to consist of a mixture of chain and ring units with an expected decrease of the amount of rings with rising temperature above T_g .^{44,45} Dembovsky⁴⁶ concluded from quantum chemical data that there is a growing number of four-fold coordinated Se (over 10% at T_g) with rising temperature. It was suggested that this could play a role in the high temperature range (for $T/T_g > 1.3$ ^{46,47}), higher than the temperature range of interest in this study. It has also been concluded from small-angle neutron scattering that the chain macromolecules of a-Se, consisting of 10^4 to 10^6 atoms up to T_g ,⁴² shorten upon increasing temperature in the liquid range.^{45,49} Rings are very likely to give a significant contribution to the resistance opposed to transverse contraction when the material is pulled in tension (recall that foams or cellular solids exhibit very low values for Poisson's ratio). Hence, the disappearance of rings is supposed to be of paramount importance on the increase in ν . The site fraction of Se-atoms building rings was estimated to lie about 0.85, 0.78,

0.66, and 0.56 at 293, 300, 350, and 400 K, respectively.⁴⁵ It is inferred from the rapid increase in Poisson's ratio that this deconstruction is very rapid within 10 K around T_g , but the fraction of ring at the onset of this abrupt weakening cannot be considered as resulting from a percolation of these units.^{50,51} Now because the interchain bonding is relatively weak (Van der Waals type), upon heating a-Se looks more and more like short $(-Se)_n$ segments embedded in a soft phase, so that shear is enhanced and both shear modulus and viscosity drop sharply.

The introduction of germanium adds to the complexity of the problem. When the selenium content exceeds 80% ($GeSe_4$, $GeSe_9$) anomalous wide-angle x-ray scattering and small-angle x-ray scattering suggest that the structure mainly consists of isolated $GeSe_4$ tetrahedra in an amorphous Se matrix.¹² A recent first principle molecular dynamics simulation on $GeSe_4$ proposes more details to the picture: 88% of Ge atoms are involved in tetrahedral $GeSe_4$ units and a few are not four-fold coordinated to Se but would form $Ge-Se_2$ and $Ge-GeSe_3$ units, while Se would form $Se-Se_2$, $Se-Se-Ge$, and $Se-Ge_2$ motifs.¹⁶ At lower selenium content, corner-sharing and edge-sharing tetrahedra are observed.^{12,18} This suggests that there are few—or less¹⁷⁻¹⁹ than expected from the stoichiometry (chain-crossing model)—Se-Se bridges between $GeSe_{4/2}$ tetrahedra, even for the $GeSe_4$ composition. This indicates the presence of Se-rich units in the structure, but not isolated, as suggested by the bimodal model. In addition, because of the relative ease for the dissociation of $GeSe_2$ units,⁵² it is anticipated that more and more homopolar bonds ($Ge-Ge$, $Se-Se$) will form upon heating above T_g , giving to the network a more and more chemically heterogeneous nature. Neutron-scattering studies^{53,54} conducted on liquid samples from the Ge_xSe_{1-x} system at temperature above 900 K confirmed the disappearance of heteropolar $Ge-Se$ bonds with increasing temperature in the liquid range and indicate that the intermediate range order becomes less significant while the average coordination number $\langle n \rangle$ does not seem to change. Besides, although weak regions develop in the glass network, $GeSe_{4/2}$ tetrahedral units are not much affected. These units clearly oppose transverse contraction under tensile loading and are responsible for a relatively low value and for a weak temperature sensitivity of ν in the presence of significant amount of germanium. Our $\nu(T)$ data also suggest little change in the network cross-linking degree in the case of $GeSe_3$, $GeSe_4$, and Ge_3Se_7 compositions and are thus consistent with these structural observations. Furthermore, the fact that $GeSe_3$ and $GeSe_4$ compositions behave very similarly (normalized elasticity and viscosity curves are almost superimposed) would support either the existence of an intermediate phase controlling the behavior in this composition range ($x = 0.2$ to 0.25),⁵⁵ or the possibility that for Ge content (over 20 at.%), the Se-rich phase are progressively taking over the $GeSe_2$ units in controlling the properties of the glasses. This is in agreement with a recent ⁷⁷Se NMR study⁵⁶ suggesting few bond exchanges between Se rich domains and $GeSe_2$ units and larger mobility of Se-Se sites.

B. Thermal-activation parameters and deformation mechanism

The height of the free-activation energy, ΔG_a , for the viscous-flow process is much lower than any interatomic bond-

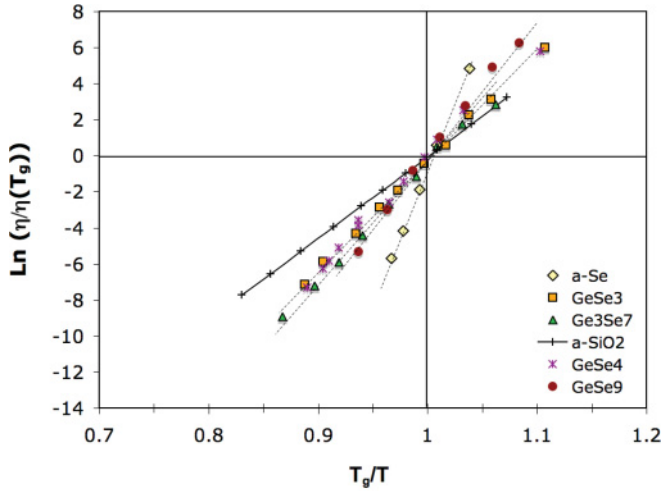


FIG. 4. (Color online) T_g -scaled logarithm of viscosity from which the fragility index is straightforwardly derived from the slope of the linear intercepts in the transition range. The scaling parameter used here is the temperature corresponding to a viscosity of 10^{12} Pa · s.

ing energy (264, 330, and 484 kJ · mol⁻¹ for U_oGe-Ge, U_oSe-Se, and U_oSe-Ge, respectively⁵¹). This suggests that deformation proceeds by shear along the soft regions in between stiffer structural units. The larger the selenium content is, the larger the activation entropy (ΔS_a) induced by the flow process and the fragility index (m) become (Fig. 4 and Table II). This is in agreement with the work published by Nemilov,³⁸ which already suggested a strong correlation between ΔS_a and m . As long as stress effects on viscosity can be neglected (i.e., flow remains Newtonian), ΔS_a reflects the temperature dependence of the energy barrier and is chiefly related to thermally induced changes of the shear modulus [see Eq. (7)]. Therefore the large entropy contribution and the abrupt entropy change above T_g (Fig. 5) in the case of a-Se corroborates the steep softening observed in the same temperature range.

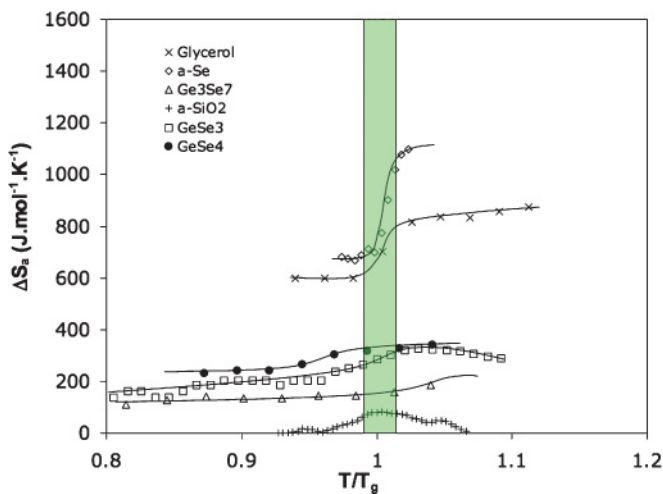


FIG. 5. (Color online) Activation entropy as calculated from (7) accompanying the shear viscous-flow process in the transition range for glasses with different degrees of network cross-linking.

1. Amorphous selenium

There are obviously some dramatic microscopic events responsible for the rapid softening and increase of the activation entropy at T_g . Misawa *et al.*⁴⁵ studied the temperature dependence and the energetics of the ring to chain transition in a-Se. In particular these authors intended to estimate the entropy increase associated with the fragmentation of the Se chains. The following expression was derived for the entropy increase

$$\Delta S = R \ln \left[\left(\frac{n_c}{q} \right)^q \frac{1}{f_c^{2q-1} (q-1)! \xi^q} \right], \quad (10)$$

where n_c is the number of Se atoms in the chain before fragmentation and q is the number of Se-Se bond disruptions (n_c/q is the average number of atoms in the fragments), f_c is the fraction of chains (versus rings), and ξ is a constant calculated to be $4.2 \cdot 10^{-3}$. Using their data at T_g ($n_c/q \sim 5.10^5$, $f_c \sim 0.22$) an entropy change of ~ 1100 J · mol⁻¹ · K⁻¹ (Fig. 5) would correspond to six cuts in a chain. At 350 K ($T/T_g \sim 1.12$), with $n_c/q \sim 2.10^5$ and $f_c \sim 0.34$, the same entropy change corresponds to eight cuts. Just below T_g the number of cuts falls down to approximately 4 ($\Delta S = 700$ J · mol⁻¹ · K⁻¹, $n_c/q \sim 10^6$, $f_c \sim 0.15$). It would be very interesting to study the changes of the chain length and chains-to-rings fraction *in situ* at high temperature under stress to determine whether viscous flow affects these processes or not. At higher temperature the activation entropy is expected to decrease as the system gains more and more ergodicity. This is indeed predicted by Eq. (8): As T increases and μ decreases toward zero, ΔS_a tends toward $1/T$. It is noteworthy that glasses such as glycerol and selenium consisting of chain-like structural units experience a large change in ΔS_a in the transition range, whereas weak changes are observed in more cross-linked glasses, such as a-SiO₂.

2. Germanium selenide glasses

We observed a decrease of the temperature sensitivity of the viscosity (ΔH_a) with an increase of the germanium content up to 20% (GeSe₄). Then ΔH_a increases and reaches a value for Ge₃Se₇ higher than for GeSe₉. Our data corroborate previously reported data on similar glasses³² and concluded to a U-shape curve for ΔH_a as a function of the germanium content, with a decrease for $\langle n \rangle$ below 2.4 and an increase above this value and up to the GeSe₂ composition. The activation energy for enthalpy relaxation shows also an identical U-shape.¹⁴ However, one should keep in mind that the free-activation enthalpy ΔG_a is the relevant parameter of the flow process and is systematically smaller than the apparent energy ΔH_a . The discrepancy is especially large for a-Se (41 kJ · mol⁻¹ and 369 kJ · mol⁻¹ for ΔG_a and ΔH_a , respectively). A monotonic increase of ΔG_a with the germanium content, from 95 kJ · mol⁻¹ for a-Se to 183 kJ · mol⁻¹ for Ge₃Se₇, is predicted from the simple model proposed by Nemilov.³⁸ These values are in reasonable agreement with those we obtained taking advantage of our high temperature elasticity data (41 kJ · mol⁻¹ and 144 kJ · mol⁻¹, respectively). This monotonic trend might simply reflect the fact that an increase of the germanium content results in an increase of the elastic moduli and thus to an increase of the volume density of

energy (1st Grüneisen rule). The height of the energy barrier for viscous flow being of an overwhelming part of elastic origin, a monotonic increase of ΔG_a with the germanium concentration follows. Therefore, the unexpected U-shape curve depicted by ΔH_a as a function of the germanium content is simply attributable to a dramatic composition-dependence of the activation entropy. The relatively strong temperature sensitivity of the viscosity at large germanium contents, with a fragility index remaining as large as 27 for both GeSe_3 and Ge_3Se_7 , stems from the fact that the breakdown of the cross-linked network structure (disappearance of the medium range order) above T_g favors shear in between structural units, which are no more strongly interconnected. Eventually, glasses containing at least 40% germanium (Ge_2Se_3) are likely to consist of Ge-rich clusters in a selenium matrix and might show a fragility index close to the one of pure a-Se, as observed by Senapati *et al.*³² Our understanding of the incidence of the composition and structure of germanium selenide glasses on their elastic and viscous deformation is illustrated by the schematic drawings depicted in Fig. 6 and corresponding to the following situations: (a) In glassy selenium eight-member rings chiefly predominate over chains. When the temperature approaches the transition range [Fig. 6(b)] rings progressively disappear to the benefit of chains, and Poisson's ratio starts to increase because of the loss of the resistance against transverse shrinkage. Above the transition the fragmentation of the chains becomes more and more significant and some alignment of the fragments may be observed [Fig. 6(c)]. The higher the temperature becomes, the smaller the fraction of rings and the number of atoms per Se chains [Fig. 6(d)] are. The addition of germanium results in the formation of relatively

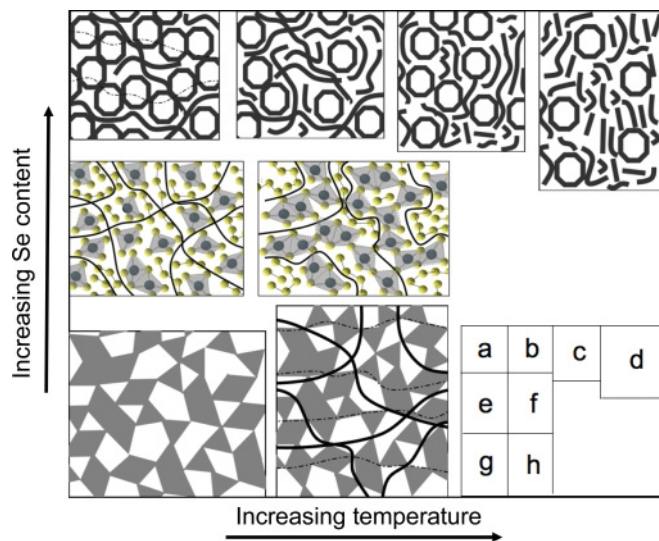


FIG. 6. (Color online) Schematic drawing illustrating the thermally induced changes and the consequences on the elastic and viscous behaviors. Dashed lines show transverse load bearing arms, which oppose lateral contraction upon pulling along a vertical axis. Solid lines show possible regions for easy shear slip. The loading axis has to be imagined vertical in the plane of the figure. (a) to (d): a-Se, with increasing temperature. (e) and (f): $\text{Ge}_x\text{Se}_{1-x}$ glasses with increasing germanium content for $x < 0.2$. (g) and (h) At high germanium content ($x \geq 0.20$), at rest and under stress.

rigid $\text{GeSe}_{4/2}$ tetrahedra. As long as the germanium content remains below 20 at.%, the glass network exhibits weak selenium-rich path for shear in-between Ge-based tetrahedra. The glass network shows up like $\text{GeSe}_{4/2}$ tetrahedra clusters with few connections with a soft amorphous selenium matrix [Fig. 6(e)]. When the germanium content is high enough, say for $x \geq 0.20$ (GeSe_4), a subnetwork of interconnected tetrahedra forms, which brings stiffness to the glass [Fig. 6(f)]. At germanium content over 25 at.% (GeSe_3), the cross-linked network provides numerous transverse stressed arms, likely to follow edge-sharing tetrahedra. Hence Poisson's ratio turns out to be quite small and to evolve little with temperature through the transition range. Nevertheless, there still remain some continuous channels between edge-shared $\text{GeSe}_{4/2}$ tetrahedra, which provide paths for the shear deformation [Fig. 6(h)]. Moreover, increasing the temperature could increase the ratio of edge-shared tetrahedra, allowing such weak channels to extend. Edwards *et al.*⁵⁷ even suggest that the corner- to edge-sharing transition could be the main process involved during shear flow and enthalpy relaxation because these three processes have similar characteristic relaxation times. Nevertheless, the two latter should involve different structural events, as evidenced by their apparent activation energies [~ 110 kJ/mol for enthalpy relaxation¹⁴ and 243 kJ/mol for shear flow in the case of GeSe_4 (Table III)]. With rising temperature, Ge-rich and Se-rich regions have the tendency to form (a growing amount of homopolar Ge-Ge and Se-Se bonds are found with increasing temperature in liquid GeSe_2 ⁵²), which is attributable to the ease for dissociation of GeSe_2 . Thus the shear viscosity drops. The activation volumes (Table III) suggest volumes corresponding to a single atom for a-Se and few atoms for GeSe_3 and Ge_3Se_7 . Although these values are certainly no more than rough indications, they support the idea that the relevant scale for flow is typically the chain link in the case of a-Se and the size of the tetrahedron when $\text{GeSe}_{4/2}$ units come into play.

V. SUMMARY AND PERSPECTIVES

We have studied the high temperature elastic behavior and the shear viscosity of germanium selenide glasses in the transition range. Young's modulus and the shear modulus were measured by means of a resonant technique in the 5- to 10-kHz range. Viscosity was measured using a displacement- and load-controlled indentation apparatus. A steep increase in Poisson's ratio (ν) starting slightly below T_g was observed for a-Se whereas little changes were noticed for GeSe_3 and GeSe_7 compositions. Since ν was found previously in a couple of independent works⁶⁻⁸ to be directly correlated to the network cross-linking degree, and to the mean coordination number in chalcogenide glasses, our results strongly suggest that over-constrained Ge-Se glasses experience minor structural changes in the transition range.

The viscous flow behavior could be well described by a pure Arrhenius-type law with a single apparent activation energy ΔH_a for the flow process in the temperature range of concern (0.8 to 1.1 T_g). The estimated values for ΔH_a are in good agreement with those reported by previous investigators in the same temperature range and show a constant decrease

with rising Ge content up to 20 at.% Ge that correlate with a minimum in reported heat flows at the glass transition. However for higher Ge contents, ΔH_a increases. We have applied the theory of thermally activated flow phenomena to analyze our data and derive the activation entropy for flow by means of both elasticity and viscosity data. It turns out that the activation entropy is very high for a-Se and decreases rapidly with rising Ge content. Consequently, the free enthalpy of the flow process is in fact much lower than ΔH_a for the Se-rich compositions. We propose that the entropy change is of an overwhelming part of elasticity origin and is intimately related to the fragmentation of the chains and, probably to a lesser extent, to the ring to chain transition. A sketch of the different events occurring in the studied glasses was drawn to describe the structural changes and the deformation mechanisms as a function of the composition. In particular special focus was made to explain the occurrence of easy-shear zones in over-constrained Ge-Se compositions, notwithstanding the weak changes of ν observed in the same temperature range.

Most structural studies on germanium chalcogenide glasses were performed either at RT or in the liquid range for $T \gg$

T_g . We feel that x-ray and neutron scattering conducted *in situ* in the transition range under stresses would be invaluable to get insight into the stress-induced structural changes and thus into the deformation process. For instance this would allow estimating possible effects of the stress on the characteristics of the structural units (namely the Se-chains conformation and length, the inter- and intratetrahedral angles, the texturation, etc.).

ACKNOWLEDGMENTS

We are indebted to Q. Coulombier and to the UMR CNRS 6226 for providing us with high-quality melt-quenched chalcogenide specimens. We are also grateful to all the people at LARMAUR who offered their valuable help to the experimental investigations. This work has been partly supported by the French Ministry of Higher Education and Research (Ph.D. grant for Yann Gueguen). We also wish to thank Prof. S.V. Nemilov (St. Petersburg State University of Information Technologies, Mechanics and Optics, St. Petersburg, Russia) and Prof. P. Salmon (University of Bath, Great Britain) for their helpful remarks on the manuscript.

*tanguy.rouxel@univ-rennes1.fr

†Present address: LIMATB, EA-4250, UBS-LORIENT, Centre de Recherche, rue de Saint Maudé – BP92116, 56321 Lorient Cedex, France.

¹J. A. Savage, *Infrared Optical Materials and Their Antireflection Coating*, edited by Adam Higlger (Adam Hilger Pub., Bristol, UK, Boston, MA, 1985).

²J. Portier, *J. Non-Cryst. Solids* **112**, 15 (1989).

³J. Lucas, in *Glasses and Amorphous Materials*, edited by J. Zarzycki, Chap. 8 (VCH, New York, 1991), pp. 457–488.

⁴A. K. Varshneya, in *Fundamentals of Inorganic Glasses* (Academic Press Inc., Boston, London, Tokyo, 1994), p. 7.

⁵C. Zwikker, ed., in *Physical Properties of Solid Materials* (Willey Interscience, New York, 1954), p. 90.

⁶B. Bridge and A. A. Higazy, *Phys. Chem. Glasses* **27**, 1 (1986).

⁷T. Rouxel, *J. Am. Ceram. Soc.* **90**, 3019 (2007).

⁸A. N. Sreeram, A. K. Varshneya, and D. R. Swiler, *J. Non-Cryst. Solids* **128**, 294 (1991).

⁹R. Böhmer and C. A. Angell, *Phys. Rev. B* **48**, 5857 (1993).

¹⁰P. Boolchand, X. Feng, and W. J. Bresser, *J. Non-Cryst. Solids* **293–295**, 348 (2001).

¹¹C. Massobrio, M. Micoulaut, and P. S. Salmon, *Solid State Sci.* **12**, 199 (2010).

¹²P. Armand, A. Ibanez, H. Dexpert, D. Bittencourt, D. Raoux, and E. Philippot, *J. Phys. IV* **2**, C2-189 (1992).

¹³B. Bureau, J. Troles, M. Le Floch, P. Guenot, F. Smektala, and J. Lucas, *J. Non-Cryst. Solids* **319**, 145 (2003).

¹⁴P. Lucas, E. A. King, O. Gulbiten, J. L. Yarger, E. Soignard, and B. Bureau, *Phys. Rev. B* **80**, 214114 (2009).

¹⁵I. T. Penfold and P. S. Salmon, *Phys. Rev. Lett.* **67**, 97 (1991).

¹⁶C. Massobrio, M. Celino, P. S. Salmon, R. A. Martin, M. Micoulaut, and A. Pasquarello, *Phys. Rev. B* **79**, 174201 (2009).

¹⁷R. Golovchak, O. Shpotyuk, A. Kozyukhin, A. Miller, and H. Jain, *J. Appl. Phys.* **105**, 103704 (2009).

¹⁸E. L. Gjersing, S. Sen, and B. G. Aitken, *J. Phys. Chem. C* **114**, 8601 (2010).

¹⁹M. Kibalchenko, J. R. Yates, C. Massobrio, and A. Pasquarello, *J. Phys. Chem. C* **115**, 7755 (2011).

²⁰C. Bernard, Ph.D thesis, University of Rennes 1 (2006) [http://tel.archives-ouvertes.fr/tel-00402562_v1/].

²¹C. Bernard, V. Keryvin, J.-C. Sangleboeuf, and T. Rouxel, *Mech. Mat.* **42**, 196 (2010).

²²T. C. T. Ting, *J. Appl. Mech.* **33**, 845 (1966).

²³M. Sakai and S. Shimizu, *J. Non-Cryst. Solids* **282**, 236 (2001).

²⁴P. Gadaud and S. Pautrot, *J. Non-Cryst. Solids* **316**, 146 (2003).

²⁵P. Gadaud, X. Milhet, and S. Pautrot, *Mater. Sci. Eng. A* **521–522**, 303 (2009).

²⁶V. Keryvin, T. Rouxel, M. Huger, and L. Charleux, *J. Ceram. Soc. Jpn.* **116**, 851 (2008).

²⁷T. Rouxel, J.-C. Sangleboeuf, M. Huger, C. Gault, and S. Testu, *Acta Mater.* **50**, 1669 (2002).

²⁸W. M. Slie, A. R. Donfor, and T. A. Litovitz, *J. Chem. Phys.* **44**, 3712 (1966).

²⁹S. V. Nemilov, *Zh. Prikl. Khim.* **37**, 1020 (1964).

³⁰R. B. Stephens, *J. Appl. Phys.* **49**, 5855 (1978).

³¹W. H. Poisl, W. C. Olivier, and B. D. Fabes, *J. Mater. Res.* **10**, 2024 (1995).

³²U. Senapati and A. K. Varshneya, *J. Non-Cryst. Solids* **197**, 210 (1996).

³³F. Q. Yang and J. C. M. Li, *J. Non-Cryst. Solids* **212**, 136 (1997).

³⁴G. Schoeck, *Phys. Status Solidi B* **8**, 499 (1965).

³⁵A. G. Evans and R. D. Rawlings, *Phys. Status Solidi B* **34**, 9 (1969).

³⁶V. K. La Mer, *J. Chem. Phys.* **1**, 289 (1933).

³⁷B. Escaig and J. M. Lefebvre, *Rev. Phys. Appl.* **13**, 285 (1978).

- ³⁸S. V. Nemilov, *J. Non-Cryst. Solids* **353**, 4613 (2007).
- ³⁹S. V. Nemilov, *J. Non-Cryst. Solids* **352**, 2715 (2006).
- ⁴⁰J. C. Dyre, N. B. Olsen, and T. Christensen, *Phys. Rev. B* **53**, 2171 (1996).
- ⁴¹J.-P. Guin, T. Rouxel, J.-C. Sangleboeuf, I. Melscoët, and J. Lucas, *J. Am. Ceram. Soc.* **85**, 1545 (2002).
- ⁴²X. Feng, W. J. Bresser, and P. Boolchand, *Phys. Rev. Lett.* **78**, 4422 (1997).
- ⁴³N. W. Tschoegl, W. G. Knauss, and I. Emri, *Mech. Time-Depend. Mat.* **6**, 3 (2002).
- ⁴⁴A. V. Tobolsky and A. Eisenberg, *J. Am. Chem. Soc.* **81**, 780 (1959).
- ⁴⁵M. Misawa and K. Suzuki, *J. Phys. Soc. Jpn.* **44**, 1612 (1978).
- ⁴⁶S. A. Dembovsky, *J. Non-Cryst. Solids* **353**, 2944 (2007).
- ⁴⁷S. Hamada, N. Yoshida, and T. Shirai, *Bull. Chem. Soc. Jpn.* **42**, 1025 (1969).
- ⁴⁸C. A. Angell, *J. Non-Cryst. Solids* **131–133**, 13 (1991).
- ⁴⁹M. Inui, S. Takeda, K. Maruyama, Y. Kawakita, S. Tamaki, and M. Imai, *Physica B* **213–214**, 552 (1995).
- ⁵⁰For instance, identifying the 8-member selenium rings to overlapping oblate ellipsoids with aspect ratios between 1/3 and 1/5 (which is roughly the width to diameter ratio of the rings according to structural studies), a percolation threshold between 0.17 and 0.23 is predicted following the theoretical analysis reported by Garboczi *et al.* (see Ref. 51). It can be inferred from a study on sulphur that the fraction of chalcogen atoms involved in rings in the temperature range where the onset of the increase of Poisson's ratio is observed is about 0.74-0.78 (see Ref. 44), i.e. still much larger than the percolation threshold. The difference would be even greater with the assumption of non-overlapping objects and would still be significant if spheres would have been considered instead of ellipsoids.
- ⁵¹E. J. Garboczi, K. A. Snyder, J. F. Douglas, and M. F. Thorpe, *Phys. Rev. E* **52**, 819 (1995).
- ⁵²P. A. G. O'Hare and A. Zywrinsky, *J. Chem. Thermodyn.* **28**, 459 (1996).
- ⁵³K. Maruyama, M. Inui, S. Takeda, S. Tamaki, and Y. Kawakita, *Physica B* **213–214**, 558 (1995).
- ⁵⁴P. S. Salmon, *J. Non-Cryst. Solids* **353**, 2959 (2007).
- ⁵⁵M. Micoulaut and J. C. Phillips, *J. of Non-Cryst. Solids* **353**, 1732 (2007).
- ⁵⁶E. L. Gjersing, S. Sen, and R. E. Youngman, *Phys. Rev. B* **82**, 014203 (2010).
- ⁵⁷T. Edwards and S. Sen, *J. Chem. Phys. B* **115**, 4307 (2011).